Tehran University of Medical Sciences Publication
https://tums.ac.ir

Iran J Parasitol

Open access Journal at
https://ijpa.tums.ac.ir

Iranian Society of Parasitology
https://isp.tums.ac.ir

Original Article

Antileishmanial Activity of Quercetin-ZnMgFe2O4 Nanostructure on *Leishmania major in Vitro*

Sahar Gheisari [1], *Mahdi Delavari [1], Iraj Salimikia [2], Ali Sobhani Nasab [3]

1. *Infectious Diseases Research Center, Kashan University of Medical Sciences, Kashan, Iran*
2. *Department of Pharmacognosy, Faculty of Pharmacy, Lorestan University of Medical Sciences, Khorramabad, Iran*
3. *Physiology Research Center, Institute for Basic Sciences, Kashan University of Medical Sciences, Kashan, Iran*

Received 15 Feb 2026
Accepted 07 Jun 2026

Keywords:
L. major;
Quercetin;
$ZnMgFe_2O_4$;
Nanoparticle;
In vitro

***Correspondence**
Email:
mdelavari1@gmail.com

Abstract

Background: Cutaneous leishmaniasis is a neglected parasitic disease prevalent in tropical and subtropical regions, caused by different species of the genus *Leishmania*. Current therapeutic options are limited due to toxicity, prolonged treatment regimens, and emerging drug resistance.

Methods: This study was conducted at Kashan University of Medical Sciences, Kashan, Iran in 2024. The antileishmanial activity of quercetin and a synthesized quercetin–$ZnMgFe_2O_4$ nanostructure was evaluated against *L. major* promastigotes *in vitro* conditions. The nanostructure was synthesized and characterized using X-ray diffraction (XRD), Fourier transform infrared spectroscopy (FTIR), and scanning electron microscopy (SEM). The antileishmanial activity was assessed by determining the mortality rate of promastigotes at different concentrations (150, 300, 450, and 600 µg/mL) of quercetin and also quercetin–$ZnMgFe_2O_4$ nanostructure. In addition, ultrastructural and nuclear alterations were examined following exposure to 150 and 600 µg/mL of both quercetin and the nanostructure.

Results: The quercetin–$ZnMgFe_2O_4$ nanostructure exhibited significantly higher inhibitory activity compared with quercetin. The mortality rates for the nanostructure were 73% and 85.9% at 150 and 600 µg/mL, respectively, compared with 42% and 81% for quercetin. Microscopic analysis revealed pronounced morphological alterations, including damage to the cell body and flagella, as well as destruction of the nucleus and kinetoplast.

Conclusion: The Quercetin_$ZnMgFe_2O_4$ nanostructure exhibited considerable antileishmanial activity against *L.major* promastigotes *in vitro*. Considering the obtained results, this nanostructure can be considered in anti-leishmanial studies and further *in vitro* and *in vivo* investigations are required to evaluate its safety and efficacy.

https://doi.org/10.18502/ijpa.v21i2.22081

Introduction

Leishmaniasis is one of the most important vector-borne parasitic diseases, with a high prevalence in tropical and subtropical regions, and is considered a major global health concern. Cutaneous leishmaniasis (CL) is caused by protozoan parasites of the genus *Leishmania*. It is estimated that 600,000 to one million new cases occur annually, of which only 200,000 are reported (1, 2). In Iran, two epidemiological forms of cutaneous leishmaniasis are present: the zoonotic form caused by L. major, and the anthroponotic form caused by *L. tropica* (2). According to the American Society of Tropical and Infectious Diseases, no ideal or universally applicable treatment for cutaneous leishmaniasis (CL) has been identified to date (3). Pentavalent antimonials, such as sodium stibogluconate (Pentostam) and meglumine antimoniate (Glucantime), remain the first-line therapies due to their availability and cost-effectiveness. However, these drugs are often associated with severe side effects, administration difficulties, species-dependent variations in susceptibility, and the emergence of drug resistance (4, 5). These limitations underscore the urgent need for alternative therapeutic strategies that are more effective ,safer, and affordable.

Quercetin (3,5,7,3',4'-pentahydroxyflavonol ;C15H10O7) is a naturally occurring flavonoid widely distributed in fruits, vegetables, medicinal plants, and tree bark. It is a yellow crystalline aglycone that is poorly soluble in water but exhibits diverse biological properties, including antioxidant, anti-inflammatory ,cardioprotective, anticancer, antimicrobial, antiviral ,immunomodulatory, and antiparasitic activities (6–10).

Previous investigations have demonstrated quercetin's ability to inhibit the growth of various *Leishmania* species through multiple mechanisms. For instance, in *L. braziliensis*, quercetin interferes with iron metabolism both directly, by acting as an iron chelator, and indirectly, by activating the Nrf2/HO-1 pathway and increasing reactive oxygen species (ROS) production, ultimately inducing apoptosis, necrosis, and parasite death (7). Similarly, quercetin has been shown to control promastigote proliferation, induce DNA damage, and inhibit both Try-R and Try-S strains of *L. tropica* (8). Additionally, quercetin suppresses the replication of promastigote and amastigote forms of *L. infantum* and *L. chagasi* by inhibiting acetylcholinesterase activity and iron chelation (9). In *L. major*, it targets key enzymes, including arginase, ribonucleotide reductase, and topoisomerase II, while also disrupting mitochondrial function (10). Moreover, quercetin treatment has been reported to trigger programmed cell death independent of proteases and increase the frequency of apoptotic neutrophils in *L. major* amastigotes (11). Studies in *L. donovani*-infected hamsters further confirmed the inhibitory effects of quercetin, including reduced splenic parasite burden and enhanced parasite clearance through ROS generation and mitochondrial disruption (12). In this study, using $ZnMgFe_2O_4$ nanoparticles as carriers for quercetin may enhance the drug's solubility, promote cellular uptake, and increase reactive oxygen species (ROS)-mediated leishmanicidal effects, thereby improving quercetin's therapeutic efficacy.

Considering the limitations of current therapies and the promising biological activities of quercetin, the present study was designed to investigate the antileishmanial activity of quercetin alone and in combination with $ZnMgFe_2O_4$ nanoparticles against the promastigote form of *L. major in vitro* conditions.

Materials and Methods

Study Design

This experimental interventional study was conducted in 2024 at Kashan University of Medical Sciences, Iran.

Synthesis of $ZnMgFe_2O_4$ nanoparticles

Briefly, 0.8 mmol of zinc nitrate, 0.2 mmol of magnesium nitrate, and 2 mmol of iron nitrate were dissolved in 30 mL of distilled water and stirred magnetically at 50 °C for 1 hour

under ultrasonic. The resulting precipitate was washed ,dried at 30 °C, and subsequently calcined at 800 °C for 3 h. The formation of the nanostructure was confirmed by the appearance of a brown powder. Structural characterization was performed using X-ray diffraction (XRD), Fourier transform infrared spectroscopy (FTIR) ,scanning electron microscopy (SEM).

Preparation of Quercetin–$ZnMgFe_2O_4$ Nanostructures

To prepare the nanostructure, 1 mmol of quercetin was dissolved in 10 mL of distilled water. An equal amount of pre-washed $ZnMgFe_2O_4$ nanoparticles (washed three times with water and methanol) was added to the solution. The suspension was stirred at 30 °C for 15 min, then cooled and stirred again at 30 °C to allow solvent evaporation and binding of quercetin onto the nanoparticle surface.

Parasite Culture

The study was conducted on promastigotes of *L. major* (strain MRHO/IR/75/ER). Parasites were initially cultured in Novy-MacNeal-Nicolle (NNN) and then maintained in RPMI-1640 medium supplemented with 10% fetal bovine serum (FBS). Promastigotes in the logarithmic growth phase were used for drug evaluation.

Promastigote Assay

Promastigotes were adjusted to a density of 1×10^6 cells/mL and seeded into 48-well plates. Parasites were treated with different concentrations (150, 300, 450, and 600 µg/mL) of quercetin or quercetin–$ZnMgFe_2O_4$ nanostructures. Untreated parasites served as the negative control. After 24 h incubation at 25 °C, the number of viable parasites was counted using a Neubauer hemocytometer under a light microscope.

Assessment of DNA Alterations by DAPI Staining

Nuclear alterations were evaluated using 4', 6-diamidino-2-phenylindole (DAPI) staining. Briefly, 24 h post-treatment, promastigotes were washed with phosphate-buffered saline (PBS) and fixed with 4% paraformaldehyde for 5 min at room temperature. Cells were washed with PBS and PBST (PBS containing 0.1% Tween-20) for 5 and 15 min, respectively. Parasites were subsequently stained with 5 µg/mL DAPI in PBS for 10 min and washed again with PBS and PBST. Slides were mounted with Permafluor and examined under a fluorescence microscope for phenotypic and nuclear changes.

Ultrastructural Analysis using Scanning Electron Microscopy (SEM)

Morphological changes were investigated 24 h after treatment. Promastigotes were washed in 0.1 M sodium cacodylate buffer (pH 7.2) and fixed in 2.5% glutaraldehyde in sodium cacodylate buffer for 2 h. Post-fixation was performed with 2% osmium tetroxide in cacodylate buffer, followed by washing with distilled water. Samples were dehydrated in graded ethanol concentrations (50%-70%) immersed in hexamethyldisilazane (HMDS), coated with gold, and observed using a JEOL 840 scanning electron microscope.

Statistical Analysis

Data were analyzed using SPSS software version 22 (IBM Corp., Armonk, NY, USA). The half-maximal inhibitory concentration (IC_{50}) was calculated, and results were expressed as mean ± standard deviation (SD). Graphs were plotted using Excel and GraphPad Prism. Statistical significance among groups was determined using one-way analysis of variance (ANOVA) followed by Tukey's post hoc test. Differences with $P \leq 0.05$ were considered statistically significant

Results

Physicochemical Characterization of the Nanostructure

X-ray Diffraction (XRD)

The X-ray diffraction (XRD) pattern of the $ZnMgFe_2O_4$ nanoparticles (Fig. 1) displays distinct diffraction peaks at 2θ values of approximately 18.6°, 30.2°, 35.5°, 43.1°, 53.7°, 57.3°, and 62.8°,

corresponding to the (111), (220), (311), (400), (422), (511), and (440) planes of the cubic spinel structure, respectively. The sharp and well-defined peaks indicate a high degree of crystallinity. No additional peaks related to impurities or secondary phases were observed, confirming the successful synthesis of the desired nanoparticles.

The average crystallite size was calculated using the Scherrer equation:

$$D = \frac{0.9\lambda}{\beta \cos\theta}$$

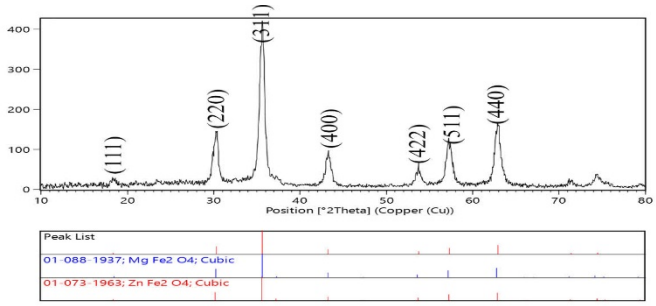

Fig. 1: X-ray diffraction (XRD) pattern of $ZnMgFe_2O_4$ nanoparticles shows distinct peaks at 2θ = 18.6°, 30.2°, 35.5°, 43.1°, 53.7°, 57.3°, and 62.8°, corresponding to the (111), (220), (311), (400), (422), (511), and (440) planes of the cubic spinel structure. These peaks confirm the high crystallinity and the successful synthesis of the intended nanoparticles.

SEM morphology of $ZnMgFe_2O_4$ nanoparticles

SEM analysis of the $ZnMgFe_2O_4$ sample reveals that the synthesized particles exhibit irregular to quasi-spherical morphologies with an average size ranging from 20 to 70 nm. The observed clustering is attributed to the high surface energy and magnetic interactions inherent to nanoscale ferrite systems (Fig. 2).

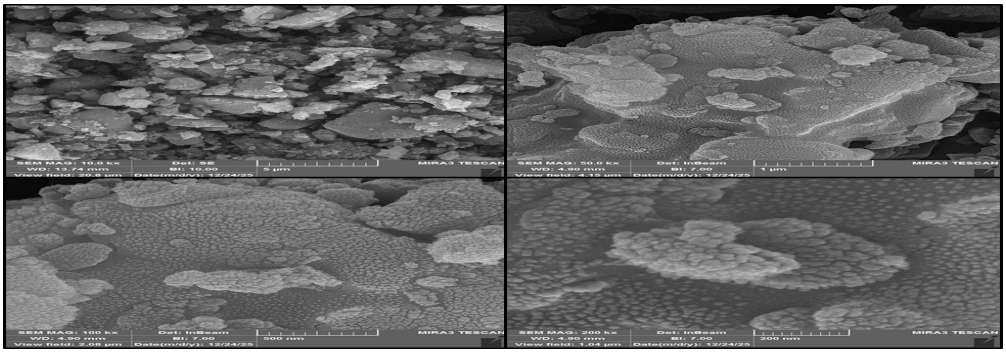

Fig. 2: Scanning electron microscopy (SEM) images of $ZnMgFe_2O_4$ nanoparticles at increasing magnifications: 5 µm, 1 µm, 500 nm, and 200 nm

Fourier-Transform Infrared Spectroscopy (FTIR)

FTIR analysis was performed to identify functional groups and confirm the loading of quercetin on the nanostructures. Spectra of pure nanoparticles and quercetin-loaded nanostructures at concentrations of 150 and 600 µg/mL are presented in Fig. 3. Characteristic bands indicate interactions between quercetin and the nanoparticle surface.

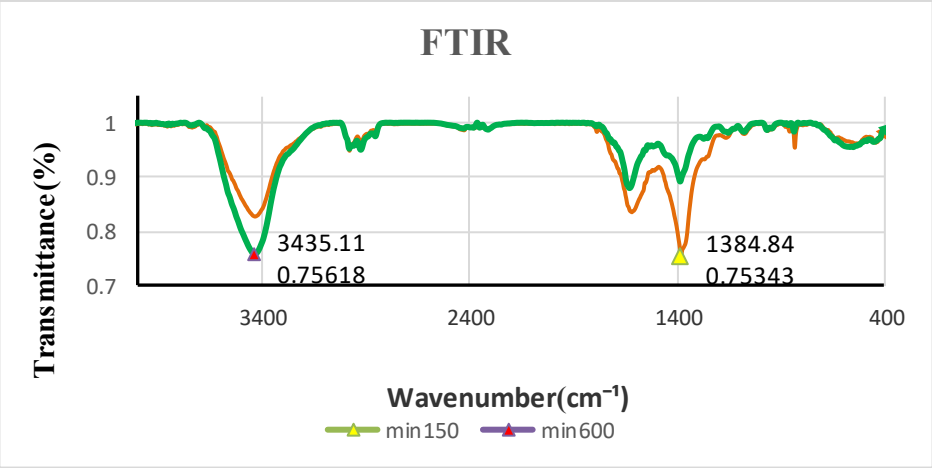

Fig. 3: FTIR spectra of the $ZnMgFe_2O_4$–quercetin nanostructure at concentrations of 150 µg/mL (orange line) and 600 µg/mL (green line) display characteristic absorption peaks corresponding to functional groups involved in quercetin loading

The broad band observed around 3435 cm^{-1} is attributed to the O–H stretching vibrations of hydroxyl groups present in quercetin molecules, as well as adsorbed water on the nanoparticle surface. The absorption band near 1384 cm^{-1} corresponds to the bending vibrations of C–O–H and the aromatic C–C bonds in quercetin. A slight shift in the position and intensity of these peaks compared to the pure nanoparticles indicates a successful interaction between quercetin molecules and the surface of $ZnMgFe_2O_4$ nanoparticles, suggesting effective drug loading.

Moreover, the bands below 600 cm^{-1} correspond to the stretching vibrations of Fe–O and Mg–O bonds within the spinel lattice, confirming the structural integrity of the ferrite core.

Therefore, the FTIR results confirm the successful loading of quercetin onto the $ZnMgFe_2O_4$ nanostructure and the formation of interfacial interactions between the organic (quercetin) and inorganic (spinel ferrite) phases.

Effect of Quercetin on L. major Promastigotes

Treatment of *L. major* promastigotes with quercetin at concentrations of 150, 300, 450, and 600 µg/mL for 24 h showed a dose-dependent inhibition of parasite viability. The percentages of cell death at these concentrations were 42%, 60%, 68%, and 81%, respectively, with the greatest growth inhibition observed at 600 µg/mL.

Effect of Quercetin–$ZnMgFe_2O_4$ Nanostructure on L. major Promastigotes

The quercetin-loaded nanostructure exhibited significantly stronger anti-leishmanial activity compared to quercetin. The percentage of promastigote death at concentrations of 150, 300, 450, and 600 µg/mL was 73%, 79%, 82%, and 85.9%, respectively, demonstrating the enhanced efficacy of the nanostructured formulation.

DNA Alterations

To evaluate nuclear changes and DNA damage, *L. major* promastigotes were treated with quercetin and quercetin–$ZnMgFe_2O_4$ at concentrations of 150 and 600 µg/mL for 24 h, then stained with DAPI. Fluorescence microscopy revealed uniform blue fluorescence and normal nuclear morphology in control cells. In contrast, treated cells exhibited scattered fluorescence with variable intensity, localized DNA condensation, the presence of small fluorescent particles, and DNA fragmentation. These effects were more pronounced at the higher concentration (600 µg/mL) (Fig. 4).

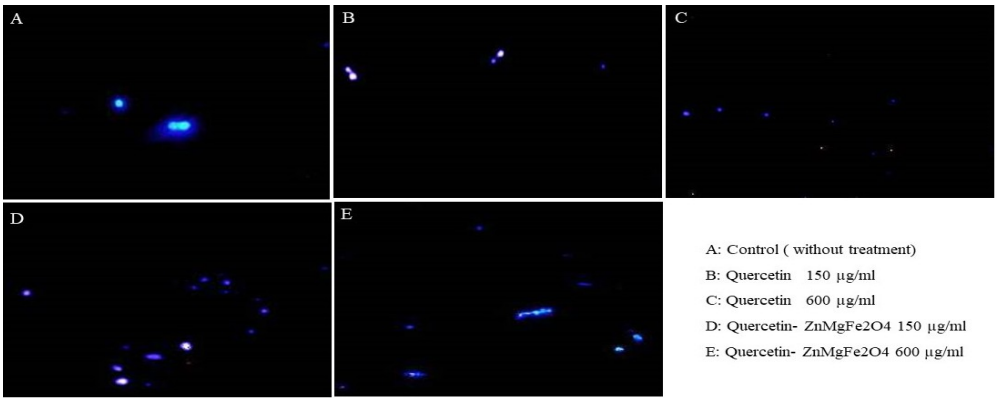

Fig. 4: Fluorescence microscopy images of *L. major* promastigotes stained with DAPI. In the control group, the nucleus and kinetoplast are clearly visible. Treatment with quercetin and quercetin–$ZnMgFe_2O_4$ nanostructure caused destruction of the nucleus and kinetoplast in a concentration-dependent manner, with more pronounced effects observed in the nanostructure-treated samples

Morphological and Ultrastructural Changes

SEM analysis of treated promastigotes revealed significant morphological alterations. Control cells exhibited smooth membranes and intact flagella, whereas treated cells showed surface wrinkling, loss of membrane integrity, flagella shortening or loss, and overall shape deformation. These changes were more pronounced in cells treated with the nanostructure at 600 µg/mL, confirming its greater anti-leishmanial potency compared to free quercetin (Fig. 5).

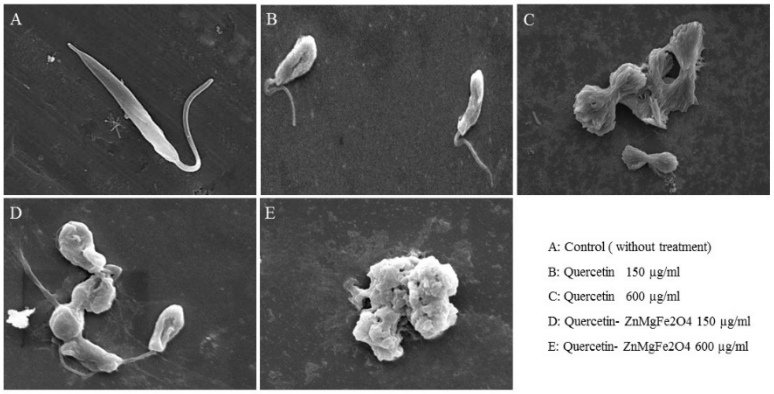

Fig. 5: Scanning electron microscopy images of *L.major* promastigotes in control and treated groups with quercetin and the quercetin–$ZnMgFe_2O_4$ nanostructures. Nanostructure exhibited significant damage to the parasite's body and flagella, with more pronounced alterations observed at higher concentrations, especially in samples treated with the nanostructure

Pharmacological Analysis

Using a four-parameter logistic (4PL) model in GraphPad Prism, pharmacological parameters were calculated. The IC50 values for quercetin and quercetin–$ZnMgFe_2O_4$ nanostructure were 157 µg/mL and 49 µg/mL, respectively, indicating greater efficacy of the nanostructure. The Emax values were 81% for quercetin and 85.9% for the nanostructure.

Overall Comparison

Collectively, quercetin–$ZnMgFe_2O_4$ exhibits stronger anti-leishmanial activity at all tested concentrations, with a lower IC50 compared to free quercetin. Loading quercetin onto the

nanostructure significantly enhances its efficacy against *L. major* promastigotes.

Discussion

The quercetin alone exhibits significant anti-parasitic effects on both promastigotes and intracellular amastigotes of *Leishmania* species. Specifically, the IC_{50} of quercetin against *L. major* promastigotes and intracellular amastigotes was reported to be 0.27 and 0.85 μM, respectively (13). In another study, the IC_{50} values of quercetin, quercitrin and isoquercitrin for recombinant arginase from *L. amazonensis* were estimated at 3.8, 10 and 4.3 μM, respectively (14). Moreover, the anti-leishmanial mechanism of quercetin against intracellular amastigotes of *L.amazonensis* was reported with an IC_{50} of 31.4 μM (15). Laboratory findings also indicated that quercetin exhibited an IC_{50} of 84.65 μg/mL against *L.donovani*, inducing nitric oxide production, apoptosis, and DNA damage, ultimately leading to parasite death (16). Furthermore, quercetin demonstrated significant inhibitory activity against other protozoan parasites. The IC_{50} values for *Babesia bovis*, *B. bigemina*, *B. caballi*, and *Theileria equi* were 8, 7, 5, and 4 nM, respectively (17). Against *Plasmodium falciparum*, quercetin showed IC_{50} and IC_{90} values of 6.9 and 11.4 μg/mL, respectively (18). For *Trypanosoma cruzi*, quercetin exhibited an IC_{50} of 142 μM through GAPDH inhibition (19), and for *T. brucei*, as a hexokinase inhibitor, the IC_{50} was 4.1 ± 0.8 μM (20).

Nano carriers enhance antileishmanial efficacy through improved drug delivery, increased cellular uptake and induction of parasite apoptosis in macrophage-hosted systems. Moreover, *in vivo* studies in BALB/c mice have confirmed that such nanostructures can significantly reduce lesion progression and parasite load compared to free drugs (21). In agreement with these findings, the present study demonstrated that the quercetin–$ZnMgFe_2O_4$ nanostructure exhibits potent inhibitory activity against *L. major* promastigotes under *in vitro* conditions, supporting the potential of nanotechnology-based strategies in the treatment of cutaneous leishmaniasis. The IC_{50} of the quercetin–$ZnMgFe_2O_4$ nanostructure in the present study was significantly lower than these reported values, demonstrating enhanced anti-leishmanial efficacy and highlighting the potential novelty of this nanostructure for the development of innovative therapeutic strategies against leishmaniasis. The incorporation of quercetin into the $ZnMgFe_2O_4$ nanostructure not only enhanced its anti-leishmanial activity but also improved its stability and bioavailability compared to free quercetin. Importantly, both the $ZnMgFe_2O_4$ nanoparticle itself and the quercetin–$ZnMgFe_2O_4$ nanostructure represent novel entities that have not been previously investigated for anti-leishmanial activity. The unprecedented combination of quercetin and $ZnMgFe_2O_4$ nanoparticles provides a promising platform for the development of next-generation anti-leishmanial therapies. These findings are in agreement with previous reports regarding the anti-leishmanial effects of nanoparticles (22–31).

In recent years, the application of nanomaterials in the treatment of parasitic diseases, particularly leishmaniasis, has attracted growing attention as an innovative and efficient therapeutic approach. Metallic and hybrid nanostructures can enhance the anti-leishmanial efficacy of drugs through mechanisms such as improved macrophage uptake, induction of apoptosis in parasites, and stimulation of host cellular immune responses. For instance, Tellurium Oxide (TeO2) Nanorods, silver nanoparticles, magnetic metal–organic frameworks (MBMOFs), and lipid nanocarriers containing artemether or amphotericin B have shown promising *in vitro* and *in vivo* results by reducing lesion size and parasite burden (22,25-27). Similarly, silver, magnesium oxide, calcium oxide, and calcium phosphate nanoparticles, either alone or in combination with anti-parasitic agents, have displayed potent leishmanicidal activity with lower cytotoxicity compared to free

drugs (23, 27–29, 31). These findings strongly suggest that nanostructured materials can serve as effective and targeted drug delivery systems to improve the therapeutic index of conventional anti-leishmanial compounds. In agreement with these reports, the present study demonstrated that the Quercetin_$ZnMgFe_2O_4$ nanostructure exhibits significant anti-leishmanial activity, supporting its potential as a novel and safe nanoformulation for the treatment of cutaneous leishmaniasis.

Quercetin, as a widely used flavonoid, possesses multiple pharmacological properties, including antioxidant, anti-inflammatory, antiparasitic, antiviral, and antibacterial activities (6, 10, 20, 32, 33).

Previous studies have shown that quercetin can affect protozoa such as Amoebae, *Plasmodium*, and *Trypanosoma* species (18, 19, 34). However, its therapeutic application is limited by low aqueous solubility and rapid degradation (35). In a clinical trial, the efficacy of two oral phytosome-formulated quercetin doses (100 and 200 mg) was compared with a single 500 mg dose of unformulated quercetin. Encapsulation within phytosomes increased bioavailability by approximately fifty-fold relative to standard or free formulations (36).

Similarly, enzymatically modified isoquercitrin (EMIQ) demonstrated up to 40-fold higher absorption (Cmax) than quercetin and reached peak plasma concentration within 15 min, suggesting enhanced activity and a broader therapeutic spectrum (37).

In the present study, loading quercetin onto the magnetic $ZnMgFe_2O_4$ nanostructure improved both its stability and bioavailability.

The use of metal nanoparticles enhances drug permeability and anti-leishmanial efficacy through mechanisms such as increased generation of reactive oxygen species (ROS), disruption of the plasma membrane, induction of oxidative stress, and ultimately apoptosis. Consistently, DAPI staining in this study revealed DNA fragmentation and pronounced nuclear alterations, indicative of apoptosis in promastigotes. Similar observations have been reported in previous investigations using metal nanoparticles or plant-derived compounds (23–25).

Findings from scanning electron microscopy (SEM) further confirmed marked morphological damage to the parasites. Observed alterations included cell rounding, flagella loss, and membrane surface irregularities. These morphological changes likely reflect compromised membrane integrity and increased permeability.

Despite these promising findings, this study has limitations. First, the investigation was restricted to the promastigote form *in vitro* conditions. Future studies should evaluate the efficacy of the nanostructure against amastigotes in animal models. Second, more in-depth molecular analyses, such as the assessment of apoptosis- and oxidative stress-related gene expression, are warranted.

Conclusion

The quercetin–$ZnMgFe_2O_4$ has significant effects on *L. major* promastigotes. Further *in vitro* and *in vivo* studies are recommended to advance its potential application in leishmaniasis treatment.

Ethical Approval

This study was approved by the Ethics Committee of Kashan University of Medical Sciences and Health with the reference number IR.KAUMS.MEDNT.REC.1402.126

Acknowledgements

This project was financially supported by Kashan University of Medical Sciences, Iran. (Project No. 402080).

Conflict of interest

The authors declare that there is no conflict of interests.

References

1. The World Health Organization Leishmaniasis Fact sheet. [(accessed on 4 January 2022)]. Available online: https://www.who.int/news-room/fact-sheets/detail/leishmaniasis.
2. Razavi MR, Shirzadi MR, Mohebali M, et al. Human Cutaneous Leishmaniosis in Iran, Up to Date-2019. J Arthropod Borne Dis. 2021;15(2):143–51.
3. Aronson N, Herwaldt BL, Libman M, et al. Diagnosis and Treatment of Leishmaniasis: Clinical Practice Guidelines by the Infectious Diseases Society of America (IDSA) and the American Society of Tropical Medicine and Hygiene (ASTMH). Clin Infect Dis. 2016; 15;63(12):1539-1557.
4. Blum J, Desjeux P, Schwartz E, et al. Treatment of cutaneous leishmaniasis among travellers. J Antimicrob Chemother. 2004;53(2):158–66.
5. Aronson NE, Joya CA. Cutaneous Leishmaniasis: Updates in Diagnosis and Management. Infect Dis Clin North Am. 2019;33(1):101–17.
6. Batiha GE, Beshbishy AM, Ikram M, et al. The Pharmacological Activity, Biochemical Properties, and Pharmacokinetics of the Major Natural Polyphenolic Flavonoid: Quercetin. Foods. 2020;9(3):374
7. Cataneo AHD, Tomiotto-Pellissier F, Miranda-Sapla MM, et al. Quercetin promotes antipromastigote effect by increasing the ROS production and anti-amastigote by upregulating Nrf2/HO-1 expression, affecting iron availability. Biomed Pharmacother. 2019:113:108745.
8. Mehwish S, Khan H, Rehman AU, et al. Natural compounds from plants controlling leishmanial growth via DNA damage and inhibiting trypanothione reductase and trypanothione synthetase: an *in vitro* and in silico approach. 3 Biotech. 2019;9(8):303.
9. Vila-Nova NS, Morais SM, Falcão MJC, et al. Leishmanicidal and cholinesterase inhibiting activities of phenolic compounds of *Dimorphandra gardneriana* and *Platymiscium floribundum*, native plants from Caatinga biome. Pesqui Vet Bras. 2012;32(11):1164–8.
10. Mohajeri M, Saghaei L, Ghanadian M, et al. Synthesis and *In vitro* Leishmanicidal Activities of Six Quercetin Derivatives. Adv Biomed Res. 2018;7(1):64.
11. Memariani H, Memariani M, Ghasemian A. Quercetin as a Promising Antiprotozoan Phytochemical: Current Knowledge and Future Research Avenues. Biomed Res Int. 2024;2024.
12. Alanazi AD, Said M Ben. Plant Bioactive Ingredients in Delivery Systems and Nanocarriers for the Treatment of Leishmaniasis: An Evidence-Based Review. Iran J Parasitol. 2022;17(4):458-72.
13. Oryan A, Bemani E, Bahrami S. Anti-leishmanial, immunomodulatory and anti-oxidative activity of quercetin against cutaneous leishmaniasis caused by *Leishmania major*. Asian Pac J Trop Biomed. 2023;13(1):26–34.
14. Da Silva ER, Maquiaveli C do C, Magalhães PP. The leishmanicidal flavonols quercetin and quercitrin target *Leishmania* (*Leishmania) amazonensis* arginase. Exp Parasitol. 2012;130(3):183–8.
15. Fonseca-Silva F, Inacio JDF, Canto-Cavalheiro MM, et al. Reactive oxygen species production by quercetin causes the death of *Leishmania amazonensis* intracellular amastigotes. J Nat Prod. 2013;76(8):1505–8.
16. Mehwish S, Varikuti S, Ali Khan M, et al. Bioflavonoid-Induced Apoptosis and DNA Damage in Amastigotes and Promastigotes of *Leishmania donovani*: Deciphering the Mode of Action. Molecules. 2021;26(19):5843.
17. AbouLaila M, Abdelaziz A, Rizk M, et al. Evaluation of the *in vitro* and *in vivo* inhibitory effects of quercetin on the growth of *Babesia* and *Theileria* parasites. Damanhour J Vet Sci. 2019;2(1):23–7.
18. Khalid SA, Farouk A, Geary TG, et al. Potential antimalarial candidates from African plants: and *in vitro* approach using *Plasmodium falciparum*. J Ethnopharmacol. 1986;15(2):201–9.
19. Freitas RF, Prokopczyk IM, Zottis A, et al. Discovery of novel *Trypanosoma cruzi* glyceraldehyde-3-phosphate dehydrogenase inhibitors. Bioorg Med Chem. 2009; 17(6):2476–82.
20. Tasdemir D, Kaiser M, Brun R, et al. Antitrypanosomal and antileishmanial activities of flavonoids and their analogues: *in vitro*, *in vivo*, structure-activity relationship, and quantitative structure-activity relationship studies. Antimicrob Agents Chemother. 2006;50(4):1352–64.
21. Mohebali F, Aghabarari B, Vaezi MR, et al. Biomacromolecule chitosan carrying meglumine

antimoniate coated on a silver/polyurethane nanostructure as a wound dressing: Therapeutic efficacy on cutaneous leishmaniasis caused by *Leishmania major* in BALB/c mice. Int J Biol Macromol. 2025;307(Pt 2).

22. Tavakoli P, Ghaffarifar F, Delavari H, et al. Synthesis of Tellurium Oxide (TeO2) Nanorods and Nanoflakes and Evaluation of Its Efficacy Against *Leishmania major In vitro* and *In vivo*. Acta Parasitol. 2022;67(1):143–52.
23. Ghaffari AD, Barati M, KarimiPourSaryazdi A, et al. *In vitro* and *in vivo* study on antiprotozoal activity of calcium oxide (CaO) and magnesium oxide (MgO) nanoparticles on promastigote and amastigote forms of *Leishmania major*. Acta Trop. 2023;238 :106788.
24. Saleh F, Kheirandish F, Abbasi M, et al. Comparison of biosynthetic zinc oxide nanoparticle and glucantime cytotoxic effects on *Leishmania major* (MRHO/IR/75/ER). J Basic Microbiol. 2024;64(5): e2300490.
25. Rahnama V, Motazedian M, Mohammadi-Samani S, et al. Artemether-loaded nanostructured lipid carriers: preparation, characterization, and evaluation of *in vitro* effect on *Leishmania major*. Res Pharm Sci. 2021;16(6):623–33.
26. Abazari R, Mahjoub AR, Molaie S, et al. The effect of different parameters under ultrasound irradiation for synthesis of new nanostructured Fe3O4@bio-MOF as an efficient anti-leishmanial *in vitro* and *in vivo* conditions. Ultrason Sonochem. 2018;43:248–61.
27. Saryazdi KA, Dalimi A, Sadeghi SH, et al. Effects of silver nanoparticle based on ginger extract on *Leishmania infantum* and *Leishmania tropica* parasites: *in vitro*. Arch Razi Inst. 2024;79(2):335.
28. Chaurasia M, Singh PK, Jaiswal AK, et al. Bioinspired Calcium Phosphate Nanoparticles Featuring as Efficient Carrier and Prompter for Macrophage Intervention in Experimental Leishmaniasis. Pharm Res. 2016;33(11):2617–29.
29. Allahverdiyev AM, Abamor ES, Bagirova M, et al. Antileishmanial effect of silver nanoparticles and their enhanced antiparasitic activity under ultraviolet light. Int J Nanomedicine. 2011;6:2705–14.
30. Rodrigues JM, Croft SL, Fessi H, et al. The activity and ultrastructural localization of primaquine-loaded poly (d,l-lactide) nanoparticles in *Leishmania donovani* infected mice. Trop Med Parasitol. 1994;45(3):223–8.
31. Özel Y, Çavuş I, Yilmaz U, et al. (Investigation of Cytotoxic and Antileishmanial Activity of Hybrid Silver Nanoparticle Complexes: Potential Drug Candidates against *Leishmania* Species). Mikrobiyol Bul. 2024 (2):182-195.
32. Anand David AV, Arulmoli R, Parasuraman S. Overviews of biological importance of quercetin: A bioactive flavonoid. Pharmacogn Rev. 2016;10(20):84–9.
33. Leopoldini M, Russo N, Chiodo S, et al. Iron chelation by the powerful antioxidant flavonoid quercetin. J Agric Food Chem. 2006;54(17):6343–51.
34. Elizondo-Luévano JH, Pérez-Narváez OA, Sánchez-García E, et al. *In-Vitro* Effect of Kalanchoe daigremontiana and Its Main Component, Quercetin against *Entamoeba histolytica* and *Trichomonas vaginalis*. Iran J Parasitol. 2021;16(3):394–401.
35. Guo Y, Bruno RS. Endogenous and exogenous mediators of quercetin bioavailability. J Nutr Biochem. 2015;26(3):201–10.
36. Riva A, Ronchi M, Petrangolini G, et al. Improved Oral Absorption of Quercetin from Quercetin Phytosome®, a New Delivery System Based on Food Grade Lecithin. Eur J Drug Metab Pharmacokinet. 2019;44(2):169-177.
37. Omi N, Shiba H, Nishimura E, et al. Effects of enzymatically modified isoquercitrin in supplementary protein powder on athlete body composition: A randomized, placebo-controlled, double-blind trial. J Int Soc Sports Nutr. 2019;16(1):39.